











## The glacial geomorphology of western Dronning Maud Land, Antarctica

J. C. H. Newall <sup>a,b,c</sup>, T. Dymova<sup>a</sup>, E. Serra <sup>a,d,e</sup>, R. Blomdin <sup>a,b</sup>, O. Fredin <sup>f,g</sup>, N. F. Glasser <sup>h</sup>,  
Y. Suganuma <sup>i,j</sup>, J. M. Harbor <sup>a,b,c,k,l</sup> and A. P. Stroeven <sup>a,b</sup>

<sup>a</sup>Geomorphology & Glaciology, Department of Physical Geography, Stockholm University, Stockholm, Sweden; <sup>b</sup>Bolin Centre for Climate Research, Stockholm University, Stockholm, Sweden; <sup>c</sup>Department of Earth, Atmospheric, and Planetary Sciences, Purdue University, West Lafayette, IN, USA; <sup>d</sup>Institute of Geological Sciences, University of Bern, Bern, Switzerland; <sup>e</sup>Oeschger Centre for Climate Change Research, University of Bern, Bern, Switzerland; <sup>f</sup>Geological Survey of Norway, Trondheim, Norway; <sup>g</sup>Department of Geography, Norwegian University of Science and Technology, Trondheim, Norway; <sup>h</sup>Centre for Glaciology, Department of Geography and Earth Sciences, Aberystwyth University, Aberystwyth, UK; <sup>i</sup>National Institute of Polar Research, Tokyo, Japan; <sup>j</sup>SOKENDAI (Graduate University for Advanced Studies), Tokyo, Japan; <sup>k</sup>Department of Geography, University of Montana, Missoula, MT, USA; <sup>l</sup>Department of Geosciences, University of Montana, Missoula, MT, USA

### ABSTRACT

Reconstructing the response of present-day ice sheets to past global climate change is important for constraining and refining the numerical models which forecast future contributions of these ice sheets to sea-level change. Mapping landforms is an essential step in reconstructing glacial histories. Here we present a new map of glacial landforms and deposits on nunataks in western Dronning Maud Land, Antarctica. Nunataks are mountains or ridges that currently protrude through the ice sheet and may provide evidence that they have been wholly or partly covered by ice, thus indicating a formerly more extensive (thicker) ice sheet. The map was produced through a combination of mapping from Worldview satellite imagery and ground validation. The sub-metre spatial resolution of the satellite imagery enabled mapping with unprecedented detail. Ten landform categories have been mapped, and the landform distributions provide evidence constraining spatial patterns of a previously thicker ice sheet.

### ARTICLE HISTORY

Received 11 October 2019  
Revised 20 April 2020  
Accepted 23 April 2020

### KEYWORDS

Antarctica; Glacial geomorphology; Nunatak; Paleoglaciology; WorldView

## 1. Introduction


The mapping of areas currently and formerly covered by glaciers and ice sheets is a key component in reconstructing past ice extent and assessing potential future responses to a changing climate (e.g. Blomdin et al., 2016; Clark et al., 2018; Fu et al., 2012; Heyman et al., 2008; Stokes et al., 2015; Stroeven et al., 2016). With models predicting that Antarctica will contribute >1 m to global sea-level rise by 2100, and >15 m by 2500 if greenhouse gas emissions continue to increase throughout the twenty-first century (DeConto & Pollard, 2016), it is important to improve our knowledge of how Antarctic ice behaved in response to past periods of climate change. Geologically-constrained ice sheet reconstructions are critical to determining the response of Antarctic ice to changing atmospheric and ocean temperatures. This is because these ice sheet reconstructions inform numerical ice sheet models and improve their ability to predict the timing and pattern of future ice reduction and consequent sea-level rise. Dronning Maud Land (DML), particularly western DML forms the focus of our mapping because it presents a significant data gap for constraining changes in the vertical extent (and therefore ice thickness) of

the East Antarctic Ice Sheet (EAIS) (Bentley et al., 2014; Mackintosh et al., 2014). Detailed mapping of glacial deposits and landforms on nunataks – mountain summits protruding through the ice sheet surface – was performed to investigate and quantify the past vertical extent of the EAIS in this area, and to guide sample collection for cosmogenic nuclide (CN) surface exposure dating to constrain the timing of ice thickness fluctuations. The vast area and harsh environment present significant accessibility challenges, therefore the mapping has been completed predominantly by remote sensing from very high-resolution satellite imagery, together with field visits to several ground validation locations.

### 1.1. Study area and previous work

Our study region covers ~200,000 km<sup>2</sup> at the western DML margin of the EAIS (Figure 1). Detailed mapping was completed on all nunataks protruding the grounded ice sheet north of 76°S and between 16°W and the Prime Meridian (Figure 1). General ice surface features (such as blue ice areas) and larger-scale erosional landforms (such as cirques) have been mapped,

**CONTACT** J. C. H. Newall  [jennifer.newall@natgeo.su.se](mailto:jennifer.newall@natgeo.su.se)

 Supplemental data for this article can be accessed <https://doi.org/10.1080/17445647.2020.1761464>

© 2020 The Author(s). Published by Informa UK Limited, trading as Taylor & Francis Group on behalf of Journal of Maps

This is an Open Access article distributed under the terms of the Creative Commons Attribution License (<http://creativecommons.org/licenses/by/4.0/>), which permits unrestricted use, distribution, and reproduction in any medium, provided the original work is properly cited.

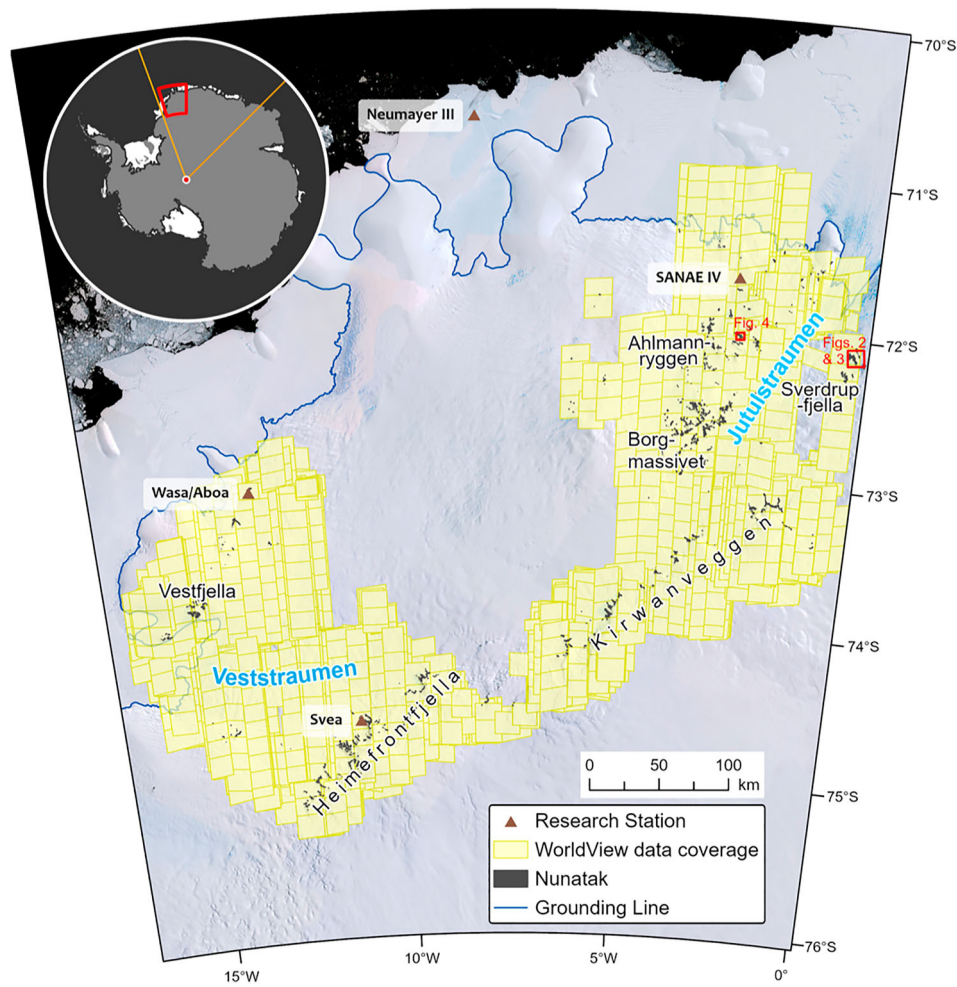


**Figure 1.** Overview of the mapped area in western Dronning Maud Land. The ice sheet grounding line is shown as the solid blue line, and the ice streams and nunatak ranges labelled are referred to in the text. The extent of WorldView satellite imagery obtained for the mapping is shown by the yellow polygons. Locations of Figures 2–4 are indicated by red rectangles. Inset map indicates the location of the mapped area within Antarctica (red box), with the red dot representing the South Pole, and the orange lines showing the defined limits of Dronning Maud Land. Basemap is the Landsat Image Mosaic of Antarctica (Bindschadler et al., 2008).

however, the focus was to perform detailed mapping of nunatak surfaces. These exposed rock surfaces comprise less than 0.2% of the study area. The *Main Map* presented here (supplementary material) builds on, and extends, mapping by Serra (2017) and Dymova (2018). We utilise new sub-metre resolution WorldView-2 and WorldView-3 satellite imagery, enabling a level of mapping detail not previously possible across such a vast region.

The ice sheet in western DML drapes an ancient passive margin escarpment which trends in a SW-NE direction, roughly coast-parallel at around 200 km inland from its grounding line. This predominantly subglacial escarpment produces substantial and complex bed relief which impedes ice flow and results in the presence of several nunatak ranges, forming the edge of the polar plateau. Downstream of the escarpment there are nunataks both in isolation and as part of additional mountain ranges (Figure 1; Vestfjella, Borgmassivet, and Ahlmannryggen). The relatively high concentration of nunataks (compared to elsewhere in the EAIS) in a sparsely investigated region

makes western DML ideal for an empirical glacial reconstruction study. The physiography of the region is described in detail in Chang et al. (2016) whose mapping of the subaerial and subglacial geomorphology of DML indicates a largely alpine landscape under the ice sheet. They could not, however, map surficial deposits on nunataks because of the coarse resolution of the available imagery (Chang et al., 2016). Numerical ice sheet modelling indicates that western DML has hosted a predominantly cold-based ice sheet since the mid-Miocene maximum  $\sim 14$  Ma (Jamieson et al., 2010) which has acted to largely preserve the alpine landscape (now largely subglacial) formed during the early Cenozoic (Näslund, 2001; Näslund et al., 2000). Macro-scale geomorphological features such as cirques were therefore likely formed prior to the inception of the EAIS  $\sim 34$  Ma, and so do not provide insight into more recent–Late Neogene and Quaternary–changes in ice sheet thickness and extent. Hence, to detect more recent modifications to the landscape we focus on mapping depositional features, such as glacially-displaced boulders (erratics), sediment cover (including

till, till veneer, talus, and regolith), and field observations of features that yield ice flow directional information, such as striations.

## 2. Methods

### 2.1. Map production

The remote sensing-based mapping of glacial geomorphology in western DML was completed using sub-metre resolution WorldView-2 (WV-2) and WorldView-3 (WV-3) satellite data. Landforms were visually identified (section 2.3) and manually digitised using ESRI ArcGIS software. An iterative approach combining remote sensing mapping and fieldwork was used to ensure interpretation integrity. The first iteration of mapping was completed ahead of the 2016–17 field season to guide sampling for CN surface exposure dating. Thus, mapping was limited to the field area of the first field season (based from Wasa and covering the Heimefrontfjella; Figure 1) and focused on sites that were realistically accessible. Detailed ground validation was completed at two locations and general observations were recorded at all sites visited during the first field campaign. The experience and insight gained during the first field season were incorporated into second generation mapping which was completed between the two field seasons (Dymova, 2018; Serra, 2017). This produced detailed coverage over the entire Ahlmannryggen and Borgmassivet nunatak ranges (Figure 1), provided a first-order reconstruction of the glacial history, and guided CN sampling for the 2017–18 field campaign. During the second field campaign detailed ground truthing was conducted at four additional locations and, again, general observations were recorded at all sites visited. The final stage of the mapping was to collate, combine, and extend the different mapping efforts across the study area. A key challenge in producing the final map product was to achieve a clear presentation of the detailed nunatak-scale mapping of landforms across such a vast study area. The map product is intended as a representation of the glacial geomorphology across western DML and readers are guided towards the shapefiles (supplementary material) in order to study in detail the glacial geomorphology of this region.

### 2.2. Data and data processing

The surficial mapping presented here uses very high-resolution commercial WorldView satellite data. WV-2 has a spatial resolution of 0.46 m in panchromatic and 1.84 m in 8 multispectral bands, while WV-3 has a spatial resolution of 0.31 and 1.24 m in the panchromatic and multispectral bands, respectively (Table 1). For identification of glacial geomorphological features, images were studied in panchromatic and 3 different

**Table 1.** Sensor band specifications and resolution for the WorldView-2 and -3 satellites.

Band	Wavelength (nm)	Resolution (WV-2)	Resolution (WV-3)
Panchromatic	450–800	0.46 m	0.31 m
Coastal	400–450	1.84 m	1.24 m
Blue	450–510	1.84 m	1.24 m
Green	510–580	1.84 m	1.24 m
Yellow	585–625	1.84 m	1.24 m
Red	630–690	1.84 m	1.24 m
Red Edge	705–745	1.84 m	1.24 m
NIR 1	770–895	1.84 m	1.24 m
NIR 2	860–1040	1.84 m	1.24 m

Note: NIR = Near infrared. The WorldView-3 satellite additionally has 8 SWIR sensors (3.7 m resolution) and 12 CAVIS – Clouds, Aerosol, (water) Vapour, Ice and Snow – sensor bands (30 m resolution), but these are omitted from the table since this data was not obtained or used in our work.

colour composites; natural, false, and modified false band combinations (Figure 2). Ice features were mapped from imagery in ‘standard false colour’ which enhances the contrast between snow and ice (Figure 2c). Surficial mapping of nunataks was completed using imagery in ‘modified false colour’ as the combination of the invisible Near-Infrared (NIR) and visible spectrum bands enhanced visual differentiation between different surface materials and geological features, especially where these differences are subtle. The modified false colour composite was particularly useful in identifying bedrock boundaries and distinguishing between different surface sediment covers (Figure 2d and f). Textures and patterns appeared most clearly in the panchromatic (Figure 2e). The ‘natural colour’ was often used to distinguish between differently coloured sediment cover and bedrock.

Given the purpose of this work, and the large storage requirement per image, WV satellite imagery was only requested for the field campaign areas and any adjacent regions containing nunataks. The extent of the WV data coverage is shown in Figure 1. In total ca. 4500 orthorectified scenes were provided, with image acquisition dates ranging from 2012 to 2016. This collection of WV images was manually filtered to select from austral summer imagery the best quality scenes to provide single-coverage over the investigation area. Almost 3000 out of the ~4500 scenes were unsuitable due to under/overexposure, the presence of striping, or cloud cover obscuring nunataks.

The reference elevation model of Antarctica (REMA) is an 8 m resolution digital elevation model (DEM) derived from WorldView imagery pairs (Howat et al., 2019) that was released in September 2018. Hence, it was not used in the first two iterations of our mapping. It was, however, utilised during the collation, combining, and checking of the mapping.

### 2.3. Glaciological features and glacial deposits

From the remote sensing we identified ten landform categories for inclusion in the mapping. The



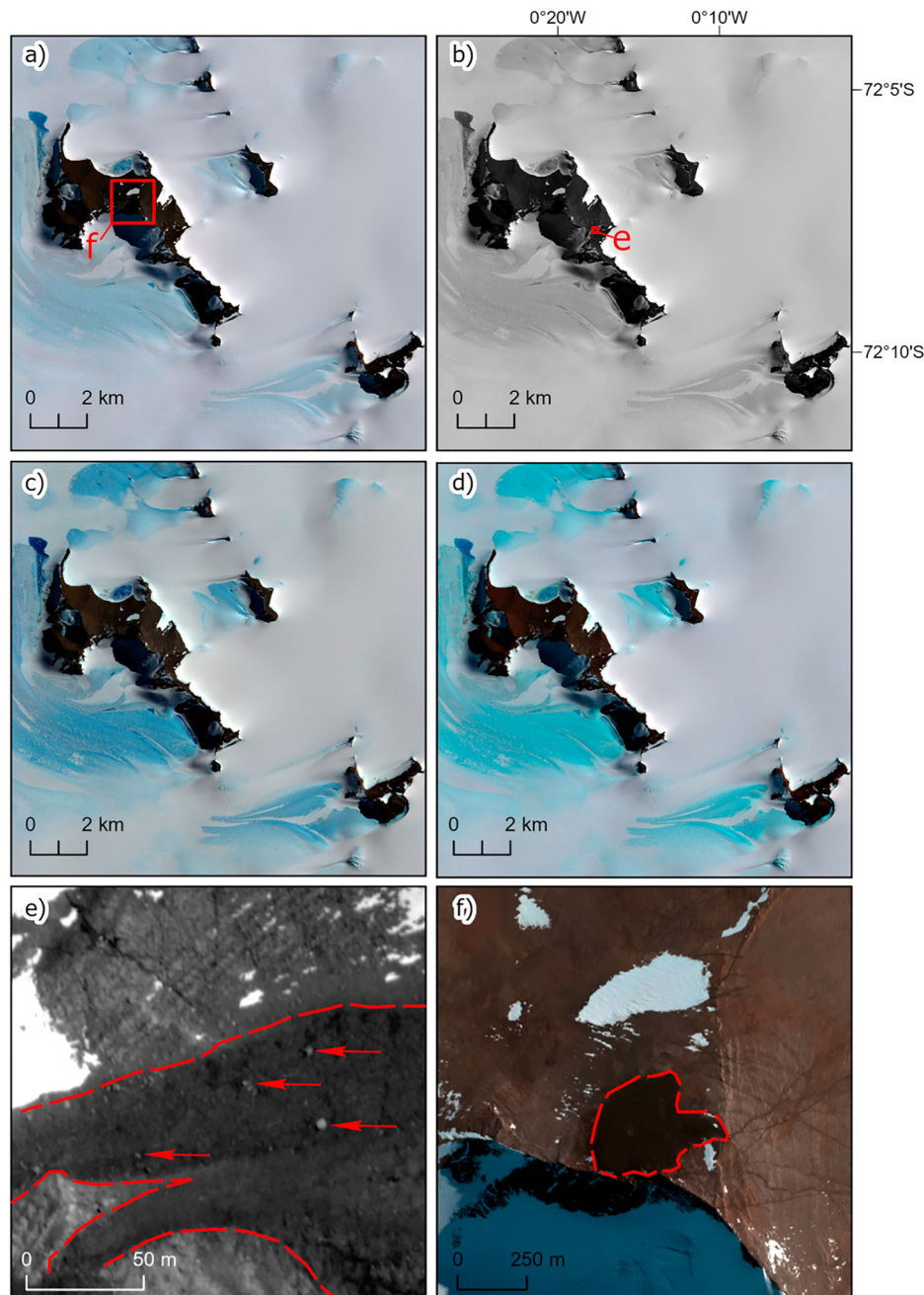


**Figure 2.** WorldView-2 imagery (© 2017 DigitalGlobe Inc.) of Sverdrupfjella (cf. Figure 1) demonstrating the different band combinations used in the mapping. The colour composites are: (a) natural colour (5,3,2), (b) panchromatic, (c) standard false colour (7,5,3), and (d) modified false colour (7,3,2). The bands utilised for each colour composite are shown in parenthesis – see Table 1 for band details. The stronger contrast between snow (white) and ice (blue), and the ability to capture subtle variations in the blue ice, made the standard false colour the optimal base for mapping ice surface features. Locations of panels e and f are indicated by red rectangles in panels b and a, respectively. The best detail is seen in panchromatic imagery, where individual boulders can be observed (e – highlighted by red arrows). The modified false colour composite proved optimal for mapping surficial features, in particular the sediment cover as it exaggerates the subtle colour differences in reds, browns, and greys (f).

identification criteria, mapping scale, optimal colour composite, and paleoglaciological significance of each mapped feature class is discussed here.

*Windscoops* are well defined, generally concave, hollows in the ice surrounding a nunatak (Figure 3). They commonly have blue ice at their base. The crest of a windscoop is flush with the ice surface, concealing a significant drop (tens of metres) towards the nunatak forming the lee side. Windscoops were mapped at scales from 1:10,000 to 1:2000 using standard false

colour composites and could be clearly identified due to the shadow they cast in the snow/ice surrounding a nunatak (Figure 3) as well as the presence of basal blue-ice areas (BIAs). Windscoops form due to channelling of the wind around a nunatak and therefore provide information on dominant wind direction and ice surface slope direction.

*Crevasses* are open cracks in the ice sheet surface that form under extensional stress (Benn & Evans, 2010). They can be tens of metres to kilometres in

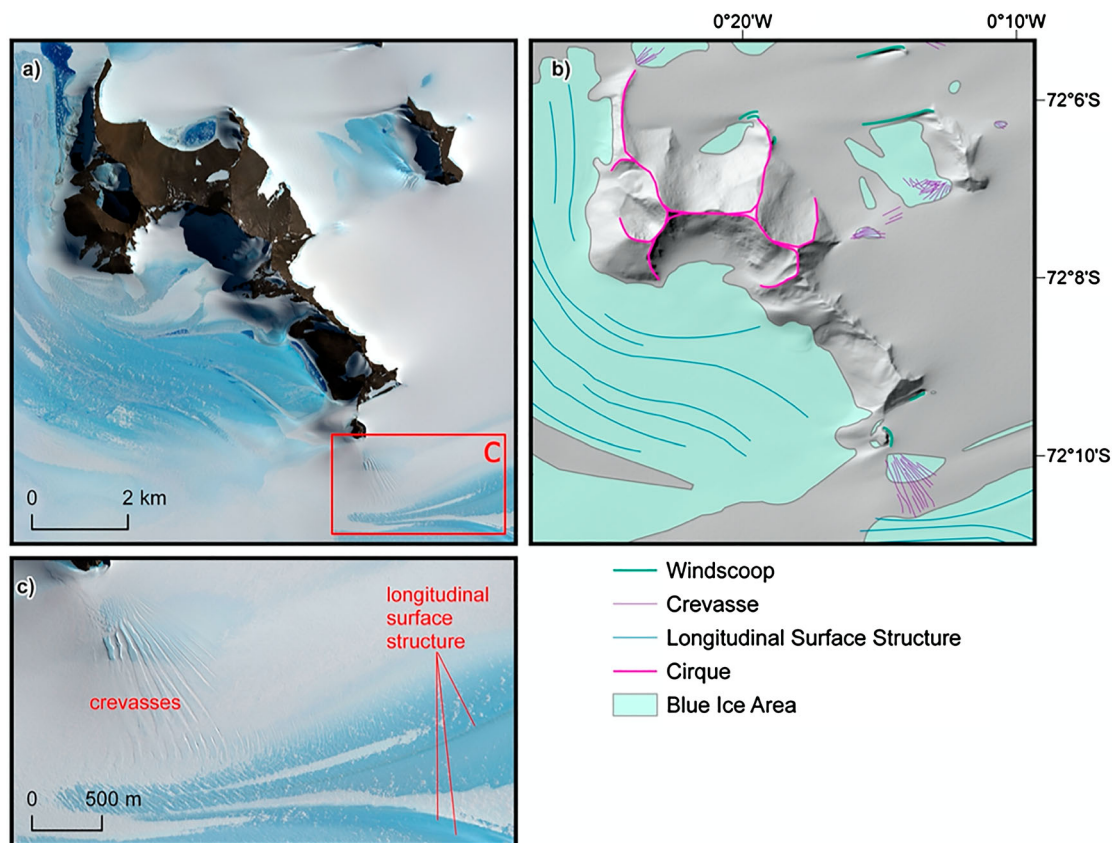


**Figure 3.** Mapping of ice surface features and cirques at Sverdrupfjella (cf. Figure 1) from WorldView-2 satellite imagery (© 2017 DigitalGlobe Inc.). (a) Sverdrupfjella in the standard false colour composite. The standard false colour emphasises bare ice, and the difference between snow and ice, and was therefore used in mapping ice features. Location of panel c is indicated by red rectangle. (b) Mapped ice features identified from (a) with a hillshade derived from the REMA DEM (Howat et al., 2019) used as background. (c) Examples of some of the smaller ice surface features, showing the detail that can be mapped from the WorldView imagery. Almost all crevasses observed were snow-filled or had partially collapsed snow bridges.

length and range from a few metres to over 50 m wide. Crevasses were mapped as individual line features at scales from 1:10,000 to 1:1500. Crevasses appeared clearest in the standard false colour composite where snow-bridges were whiter than their surroundings, and had shadows where snow-bridges had collapsed (Figure 3c). They were also distinct in the panchromatic. Crevasses are generally dynamic features which do not persist through changes in ice configuration or flow. As such the information they provide relates to present-day ice flow conditions. Additionally, and importantly, crevasses are one of the greatest safety concerns for field teams and the mapping of crevasses proved to be invaluable to route planning and field safety.

*Longitudinal surface structures (LSSs)* are flow-parallel curvilinear structures on the ice surface, often occurring as continuous subtle 1–2 m-high ridges. They typically occur within ice streams and indicate either irregularities in the bed topography or laterally compressive ice flow (Ely & Clark, 2016; Glasser & Gudmundsson, 2012). LSSs were mapped as line features at scales between 1:500,000 and 1:100,000. They typically appear as a slightly darker blue in standard false colour (Figure 3a and c), and their ridge structure

was clearest in panchromatic imagery. LSSs primarily provide information on present ice flow conditions, however, they are long-lived features and so also have the potential to provide information on changes in flow direction (Glasser & Gudmundsson, 2012).

*Blue ice areas (BIAs)* are regions of bare-ice occurring in a range of settings, though commonly on the downstream side of nunataks or on the crest of convex structures in the ice sheet surface. BIAs are wind-scoured surface ablation centres that are generally dominated by vertical ice-flow, often contain some supraglacial debris, and are renowned for concentrating meteorites (Bintanja, 1999; Fogwill et al., 2012; Spaulding et al., 2012). Whereas the ice sheet surface normally appears white in WV imagery, BIAs appear as expanses of blue ice. BIAs were best identified using the ‘standard false colour’ composite where their blue colour is distinct and the contrast between blue and white is enhanced (Figure 3). BIAs were digitised as polygons at a mapping scale of 1:10,000–1:2500. All BIAs observed were mapped, and there was no minimum or maximum size for inclusion. Small BIAs (<100 m<sup>2</sup>) were commonly found at the base of windscoops or over crevasse fields. More extensive BIAs typically occur at the base of escarpment

cliffs. They often have indistinct boundaries, in which case determining the extent of the BIA in the mapping was subjective. BIAs provide information about bed relief, past and present glacier mass balance, ice flow conditions, and predominant wind patterns. They are considered to be persistent and stable features that can survive through glacial/interglacial cycles (Bintanja, 1999; Fogwill et al., 2012; Kehrl et al., 2018; Zwinger et al., 2014).

*Boulders* are by definition any fragment of rock >25.6 cm (Wentworth, 1922), however, in our mapping we focus on large boulders (with diameters of ~1.5 m up to 10 m). Individual boulders were recognised by their three-dimensional appearance resulting from casting a shadow. They were mapped as point features at scales of 1:1000–1:500. Due to the relatively small size of the boulders they were best identified using the sub-metre resolution of the panchromatic imagery, though very large boulders can be observed in all imagery (Figure 2e). Where we have mapped large individual boulders on the summits and flanks of nunataks (where a rockfall origin can be ruled out), they are considered to be ice-transported boulders and thus indicate that the nunatak surface at this location was at some point overridden by the ice sheet (Fabel et al., 2012).

*Striations* are linear grooves on a rock surface formed as sediments embedded in the basal ice ‘scratch’ the rock surface as the ice flows over it (Benn & Evans, 2010). Striations are far too small scale to be picked up in satellite imagery. Mapped striations are therefore from field observations, with their orientation measured. Striations provide crucial information of past ice cover and orientation of flow (Stroeven et al., 2016). They were observed and measured at several sites during the field campaigns and, given their significance to glacial history, are included on the map.

*Cirques* are semi-circular depressions cut by ice in the nunatak slopes. They appear as arcuate steep cliffs forming the headwall to a bowl-shaped floor. However, cirques mapped here are ice filled and therefore only identified by the arcuate morphology of their headwalls. They range in width from a few hundred metres to kilometres. They are clearly seen in all the imagery at scales between 1:500,000 and 1:250,000. They were mapped at scales ranging from 1:50,000 to 1:6000, and digitised as line features tracing the headwall cliffs. It is generally considered that cirques indicate erosion by wet-based local glaciers (Benn & Evans, 2010; Evans & Cox, 1974), and in DML these features have often been interpreted to pre-date the inception of a permanent EAIS (Jamieson et al., 2010; Näslund, 2001; Näslund et al., 2000). However, it should be noted that Andrews and LeMasurier (1973) argue that cirque headwall retreat occurs under present-day freezing conditions in Antarctica through albedo induced freeze–thaw cycles at the headwall.

Evidence that this might be an important process was seen both in the field (direct observations of meltwater) and in the WV imagery (refrozen meltwater pools and channels). Thus the mapped cirques were likely formed during the early Cenozoic, but may still be developing slowly under present conditions in areas where seasonal meltwater is present.

*Supraglacial debris* refers to sediment lying on the surface of the ice. This includes blue-ice moraines, talus deposits, and areas containing a high concentration of scattered boulders. Supraglacial debris was easy to identify in all imagery since it is a distinctly darker speckled region on the white-blue ice surface (Figure 4). However, where there was thick supraglacial debris at or across the ice sheet-nunatak boundary it sometimes proved challenging to ascertain this boundary and therefore the limit of the supraglacial debris. Supraglacial debris was mapped as a polygon feature class at scales ranging from 1:20,000 to 1:2000. Where there was a distinct ridge or structure within the supraglacial debris this was mapped as a line feature *supraglacial debris structure* (Figure 4d). Supraglacial material was observed exclusively at the base of nunatak slopes or within BIAs (where they are mapped as overlapping units). The supraglacial material mapped on BIAs ranged from a scattering of boulders to dense deposits (Figure 4). Generally, where less than ~10% of the surface area was covered by debris, it was not included. Blue-ice moraines are considered to form by compressive ice bringing material from the base of the ice up to the surface (Fogwill et al., 2012; Hättestrand & Johansen, 2005). They therefore provide information on local ice flow patterns, in particular the locations where there is/has been vertical ice flow. Where supraglacial debris continues as a till veneer on nunatak slopes this indicates that the ice was thicker in the past.

*Sediment cover* is an amalgamation of various different types of observed surficial sediment covering nunatak bedrock (including till, till veneer, talus, and regolith) which were initially mapped as different units based on contextual assumptions (Newall et al., *in submission*). Ground validation revealed that the contextual assumptions were not reliable in differentiating these different types of sediment cover classes and they were, therefore, combined into one feature class – sediment cover. Sediment cover is observed on most nunatak plateau surfaces and non-vertical slopes and is identified primarily by a different texture and/or colour than the bedrock. Mapping of sediment cover was carried out at scales ranging from 1:5000 to 1:500, and is best identified in the modified false colour composite (Figure 2f, and Figure 4). Large concentrations of boulders are most easily identified in panchromatic imagery (Figure 2e), and denote sediment cover. Therefore, a combination of both the modified false colour and the panchromatic imagery was used



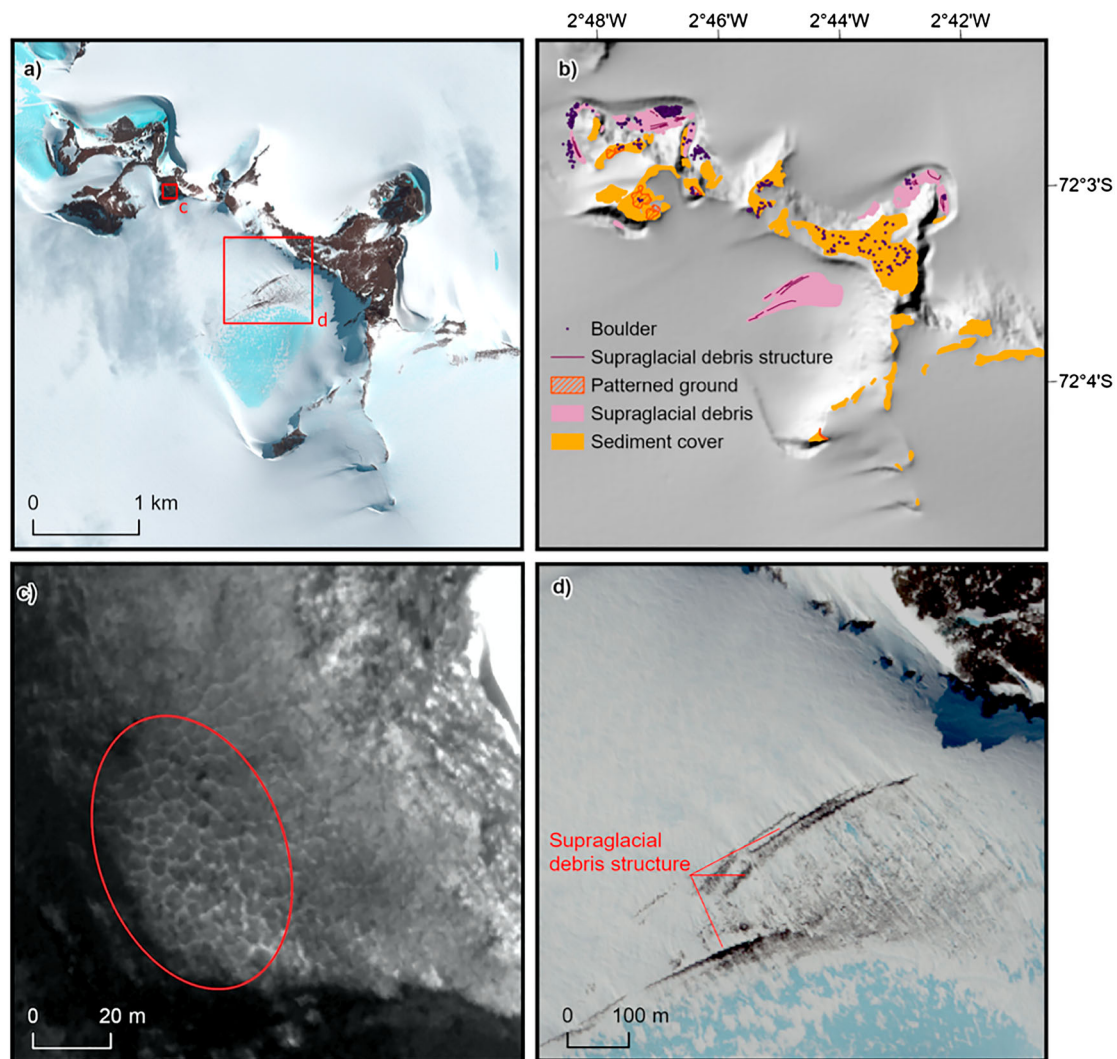


**Figure 4.** Mapping of surficial features at Grunehogna (in the Ahlmannryggen nunatak region; cf. Figure 1) from WorldView-2 imagery (©2015 DigitalGlobe Inc.). (a) Grunehogna in the modified false colour imagery. Locations of panels c and d are indicated by red rectangles. (b) The resulting mapping of surficial features from (a). Hillshade derived from the REMA DEM (Howat et al., 2019) is used for the background on which the mapping is presented. (c) and (d) show the high detail achieved in mapping from the very-high-resolution WorldView data. (c) Shows patterned ground on a nunatak plateau summit area, and (d) illustrates how supraglacial debris structures clearly stand out within the general area of supraglacial debris.

to positively identify sediment cover from bedrock. ‘Blankets’ of apparently thin sediment cover were most commonly identified, as were small ‘pockets’ of sediment between bedrock outcrops. Where sediment cover can be determined as being glacially emplaced (a till, for example), this indicates the site has been overridden by a formerly thicker ice sheet.

*Patterned ground* is marked by polygonal or striped patterns in the sediment cover found on flat plateau summits and gently sloping nunatak flanks (Figure 4a, b). Patterned ground was mapped as a polygon feature class at 1:2000–1:500 scales. It is clear in the panchromatic imagery, especially where a thin snow cover enhances the patterns (Figure 4c). A number of mechanisms have been proposed for the formation of patterned ground in glacial environments, and all require the presence of unconsolidated diamict sediments and freeze–thaw cycling (Ballantyne & Harris, 1994). The presence of patterned ground provides

information on the type of surficial material and, because the formation of patterned ground is a subaerial process and it develops gradually through periglacial processes it indicates that the nunatak surface has been exposed above ice for an extended time during which conditions were similar to, or even warmer than present (Clarhäll & Kleman, 1999; Goodfellow et al., 2008; Kleman & Stroeven, 1997; Sugden et al., 2005).

#### 2.4. Mapping consistency and completeness

The work presented here was completed over several years by multiple researchers. Smith and Wise (2007) highlight observer skill and experience as a source of bias and inconsistency in glacial geomorphological mapping. Inconsistency between mappers is also demonstrated and quantified in Hillier et al. (2015). To remove such bias, and to minimise inconsistency from numerous mappers, Newall and Stroeven were

engaged in all of the mapping activity, and Newall undertook the final map compilation which included a rigorous consistency check across the full study area. The final map presents a complete and detailed inventory of the ten mapped landforms and deposits across the study area, where they occur on or within the vicinity of a nunatak. A possible exception to mapping completeness may occur within ice surface features (crevasses, LSSs, and BIAs) where they exist distal to any nunatak, or if they occur in the pockets of the study area that are not covered by the WV satellite data acquired for the mapping (Figure 1).

### 3. Discussion

#### 3.1. Glacial history

Remote sensing and field observations both identify surficial evidence for ice cover across the full range of elevations and topographical settings (cliffs, plateaus, emergent nunataks, and ridgelines) that have been mapped. This indicates that all of the nunatak surfaces have, at some point in time, been covered by ice. The substantial spatial variation in the distribution of depositional features, and an inconsistent relationship between the presence of glacial deposits and either absolute elevation, relative elevation, or distance inland from the coast, indicate that the current complex topography in this region exerts a strong control on ice sheet configuration, dynamics, and response to external driving factors such as climate. Generally, the ice surface features are consistent with long-term stability of the flow regime. LSSs all coincide with present-day ice velocity patterns and therefore support the conclusion of Glasser et al. (2015) that the ice streams in Dronning Maud Land (and the rest of Antarctica) have been active with little to no change to flow configuration for thousands of years, possibly since the end of last glacial cycle.

#### 3.2. Ground validation

Ground validation is used to verify and validate remotely sensed mapping. By checking the mapping against ground observations, mapping accuracy can be assessed and identification criteria can be evaluated to enable the mapping of landforms to be extended regionally, beyond the sites visited. Ground truthing, conducted during the field campaigns (Newall et al., *in submission*) revealed that the contextual assumptions used to classify the different mapped units of sediment cover were not consistently correct. Using the colour composites selected for this work (section 2.2, and Table 1) it was not possible to determine the type of sediment cover from remote sensing alone. Differentiation of sediment cover proved to be challenging even in the field; experienced glacial

sedimentologists found it difficult to ascertain whether a heterogenous sediment cover was a till stripped of fines or a talus deposit sourced from heterogenous bedrock lithologies. Clast angularity can be a key criterion in classifying sediments (Lukas et al., 2013), however, across both field campaigns, almost all the clasts we encountered were angular, characteristic of both tills and regoliths stripped of fines. Therefore, clast angularity was not a reliable deterministic characteristic as to whether or not mapped sediment cover is of glacial origin. While attempts were made to map different types of sediment cover and differentiate between sediment deposits (such as till) and in-situ sediments (regolith) in the WV satellite imagery, the ground truthing showed that the methodology used here did not allow for accurate differentiation of the type of sediment cover, only to observe and map where changes in the colour and/or texture of the surficial material indicates different units of sediment cover.

The ground truthing also showed that not all mapped boulders were necessarily glacial erratics. In fact, few of the isolated boulders we mapped turned out to be true erratics (with a lithology different from the local bedrock), or showed evidence of glacial transport (e.g. striations, rounded surfaces). Boulders mapped on nunatak surfaces were considered to be quasi-erratics (ice-transported boulders) because, whereas the lithology was not strictly foreign, they could only have been transported to their particular location by ice. Hence, the mapped boulders on nunatak summits or flanks (where it can be ascertained through contextual assumptions that they do not originate from rockfall) still provide evidence of a thicker-than-present ice sheet. It should be noted that large individual boulders are also mapped on the ice surface in blue ice fields either as scattered boulders, or on supraglacial moraines. Given their proximity to the base of steep nunatak flanks they are more likely of rockfall origin as opposed to having been subglacially exhumed.

### 4. Conclusion

Detailed mapping of nunataks and nearby ice areas was completed over a 200,000 km<sup>2</sup> study area covering western Dronning Maud Land. Acquisition of sub-metre resolution WorldView satellite imagery enabled the mapping to focus on surficial features which provided information of former ice inundation. We conclude that all nunataks in western Dronning Maud Land have, at some point in time, been covered by the ice sheet and therefore provide evidence for a vertically more extensive ice sheet.

Geomorphological mapping with this level of detail was not possible previously due to the limited resolution of remote sensing products available prior to the launch of the WorldView satellites. We show that



the detection of different surficial deposits is possible, however, more work is required to positively identify the type of deposit (classification). A growing area of research is the use of very high spectral resolution satellite data in developing composition-based spectral indices (e.g. Pour et al., 2019) and weathering indices (e.g. Kanamaru et al., 2018). Future work in this direction would improve the accuracy with which we are able to classify sediment covers, however, for now ground validation is still a crucial requirement to accurately differentiate a glacial deposit from in-situ weathered bedrock.

This mapping supported the efforts of two field campaigns collecting samples for CN dating which will provide the chronological data required to build an empirical reconstruction of ice sheet thinning at the DML margin of the EAIS.

### Software

The various iterations of the mapping have been completed using ESRI ArcGIS desktop. ESRI ArcGIS 10.5 was used in the filtering of the WorldView satellite imagery scenes to create a single coverage dataset. Colour composites were dynamically applied. The final iteration of mapping, including collating and combining previous efforts and the map design and layout, used ESRI ArcGIS Pro version 2.3.

### Data

The authors have supplied the data (as ESRI shapefiles) used in the production of the accompanying map.

### Acknowledgements

This work has been funded through the MAGIC-DML consortium which is funded through various funding bodies as detailed in the funding section. Newall acknowledges the following for additional financial support; SCAR Fellowship (2015), Bolin Centre for Climate Research (Research Area 6, 2016), Stiftelsen Carl Mannerfelts Fond (2016), and Hans W:son Ahlmanns Stiftelse (2018). Logistical support was provided by the Swedish Polar Research Secretariat. Geospatial support for this work is provided by the Polar Geospatial Centre (PGC) under NSF-PLR award 1542930 and we further acknowledge the extremely helpful staff at PGC for their advice on how to optimise working with the WorldView data. We thank Heike Aps, Mike Bentley, and Jingdong Zhao for their constructive feedback, which we have used to improve the original map and manuscript.

### Disclosure statement

No potential conflict of interest was reported by the author(s).

### Funding

This work has been funded through the MAGIC-DML consortium which is supported by Stockholm University (Stroeven), Norwegian Polar Institute/NARE under Grant 'MAGIC-DML' (Fredin), the US National Science Foundation under grant number PLR-1542930 (Harbor & Lifton), Swedish Research Council under grant number 2016-04422 (Harbor & Stroeven), and the German Research Foundation (DFG), Priority Programme 1158 'Antarctic Research' under grant number 365737614 (Rogozhina & Prange).

### ORCID

J. C. H. Newall  <http://orcid.org/0000-0002-8994-1426>  
 E. Serra  <http://orcid.org/0000-0002-3049-8570>  
 R. Blomdin  <http://orcid.org/0000-0003-0306-5291>  
 O. Fredin  <http://orcid.org/0000-0002-0803-3312>  
 N. F. Glasser  <http://orcid.org/0000-0002-8245-2670>  
 Y. Suganuma  <http://orcid.org/0000-0003-3516-1317>  
 J. M. Harbor  <http://orcid.org/0000-0001-5129-0229>  
 A. P. Stroeven  <http://orcid.org/0000-0001-8812-2253>

### References

- Andrews, J. T., & LeMasurier, W. E. (1973). Rates of quaternary glacial erosion and corrie formation, Marie Byrd Land, Antarctica. *Geology*, 1(2), 75–80. [https://doi.org/10.1130/0091-7613\(1973\)1<75:ROQGEA>2.0.CO;2](https://doi.org/10.1130/0091-7613(1973)1<75:ROQGEA>2.0.CO;2)
- Ballantyne, C. K., & Harris, C. (1994). *The periglacialiation of Great Britain*. Cambridge University Press, 330 p.
- Benn, D. I., & Evans, D. J. A. (2010). *Glaciers and glaciation* (2nd ed.). Routledge, 802 p.
- Bentley, M. J., Ó Cofaigh, C., Anderson, J. B., Conway, H., Davies, B., Graham, A. G. C., Hillenbrand, C.-D., Hodgson, D. A., Jamieson, S. S. R., Larter, R. D., Mackintosh, A., Smith, J. A., Verleyen, E., Ackert, R. P., Bart, P. J., Berg, S., Brunstein, D., Canals, M., Colhoun, E. A., ... Zwartz, D. (2014). A community-based geological reconstruction of Antarctic Ice Sheet deglaciation since the Last Glacial Maximum. *Quaternary Science Reviews*, 100, 1–9. <https://doi.org/10.1016/j.quascirev.2014.06.025>
- Bindschadler, R., Vornberger, P., Fleming, A., Fox, A., Mullins, J., Binnie, D., Paulsen, S., Granneman, B., & Gorodetzky, D. (2008). The Landsat image mosaic of Antarctica. *Remote Sensing of Environment*, 112(12), 4214–4226. <https://doi.org/10.1016/j.rse.2008.07.006>
- Bintanja, R. (1999). On the glaciological, meteorological, and climatological significance of Antarctic blue ice areas. *Reviews of Geophysics*, 37(3), 337–359. <https://doi.org/10.1029/1999RG900007>
- Blomdin, R., Heyman, J., Stroeven, A. P., Hättstrand, C., Harbor, J. M., Gribenski, N., Jansson, K. N., Petrakov, D. A., Ivanov, M. N., Alexander, O., Rudoy, A. N., & Walther, M. (2016). Glacial geomorphology of the Altai and Western Sayan Mountains, Central Asia. *Journal of Maps*, 12(1), 123–136. <https://doi.org/10.1080/17445647.2014.992177>
- Chang, M., Jamieson, S. S. R., Bentley, M. J., & Stokes, C. R. (2016). The surficial and subglacial geomorphology of western Dronning Maud Land, Antarctica. *Journal of Maps*, 12(5), 892–903. <https://doi.org/10.1080/17445647.2015.1097289>
- Clarhäll, A., & Kleman, J. (1999). Distribution and glaciological implications of relict surfaces on the Ultevis plateau,

- northwestern Sweden. *Annals of Glaciology*, 28, 202–208. <https://doi.org/10.3189/172756499781821599>
- Clark, C. D., Ely, J. C., Greenwood, S. L., Hughes, A. L. C., Meehan, R., Barr, I. D., Bateman, M. D., Bradwell, T., Doole, J., Evans, D. J. A., Jordan, C. J., Monteys, X., Pellicer, X. M., & Sheehy, M. (2018). BRITICE glacial Map, version 2: A map and GIS database of glacial landforms of the last British-Irish Ice Sheet. *Boreas*, 47(1), 11–27. <https://doi.org/10.1111/bor.12273>
- DeConto, R. M., & Pollard, D. (2016). Contribution of Antarctica to past and future sea-level rise. *Nature*, 531(7596), 591–597. <https://doi.org/10.1038/nature17145>
- Dymova, T. (2018). Paleoglaciological study of the Ahlmannryggen, Borgmassivet and Kirwanveggen nunatak ranges, Dronning Maud Land, East Antarctica, using WorldView imagery. Master Thesis in Physical Geography and Quaternary Geology NKA227, Department of Physical Geography, Stockholm University, 68 p.
- Ely, J. C., & Clark, C. D. (2016). Flow-stripes and foliations of the Antarctic ice sheet. *Journal of Maps*, 12(2), 249–259. <https://doi.org/10.1080/17445647.2015.1010617>
- Evans, I. S., & Cox, N. (1974). Geomorphometry and the operational definition of cirques. *Area*, 6(2), 150–153.
- Fabel, D., Ballantyne, C. K., & Xu, S. (2012). Trimlines, blockfields, mountain-top erratics and the vertical dimensions of the last British-Irish Ice Sheet in NW Scotland. *Quaternary Science Reviews*, 55, 91–102. <https://doi.org/10.1016/j.quascirev.2012.09.002>
- Fogwill, C. J., Hein, A. S., Bentley, M. J., & Sugden, D. E. (2012). Do blue-ice moraines in the Heritage Range show the West Antarctic ice sheet survived the last interglacial? *Palaeogeography, Palaeoclimatology, Palaeoecology*, 335–336, 61–70. <https://doi.org/10.1016/j.palaeo.2011.01.027>
- Fu, P., Heyman, J., Hättestrand, C., Stroeven, A. P., & Harbor, J. M. (2012). Glacial geomorphology of the Shaluli Shan area, southeastern Tibetan Plateau. *Journal of Maps*, 8(1), 48–55. <https://doi.org/10.1080/17445647.2012.668762>
- Glasser, N. F., & Gudmundsson, G. H. (2012). Longitudinal surface structures (flowstripes) on Antarctic glaciers. *The Cryosphere*, 6(2), 383–391. <https://doi.org/10.5194/tc-6-383-2012>
- Glasser, N. F., Jennings, S. J. A., Hambrey, M. J., & Hubbard, B. (2015). Origin and dynamic significance of longitudinal structures (“flow stripes”) in the Antarctic Ice sheet. *Earth Surface Dynamics*, 3(2), 239–249. <https://doi.org/10.5194/esurf-3-239-2015>
- Goodfellow, B. W., Stroeven, A. P., Hättestrand, C., Kleman, J., & Jansson, K. N. (2008). Deciphering a non-glacial/glacial landscape mosaic in the northern Swedish mountains. *Geomorphology*, 93(3–4), 213–232. <https://doi.org/10.1016/j.geomorph.2007.02.018>
- Hättestrand, C., & Johansen, N. (2005). Supraglacial moraines in Scharffenbergboten, Heimefrontfjella, Dronning Maud Land, Antarctica – significance for reconstructing former blue ice areas. *Antarctic Science*, 17(2), 225–236. <https://doi.org/10.1017/S0954102005002634>
- Heyman, J., Hättestrand, C., & Stroeven, A. P. (2008). Glacial geomorphology of the Bayan Har sector of the NE Tibetan Plateau. *Journal of Maps*, 4(1), 42–62. <https://doi.org/10.4113/jom.2008.96>
- Hillier, J. K., Smith, M. J., Armugam, R., Barr, I., Boston, C. M., Clark, C. D., Ely, J., Frankl, A., Greenwood, S. L., Gosselin, L., Hättestrand, C., Hogan, K., Hughes, A. L. C., Livingstone, S. J., Lovell, H., McHenry, M., Munoz, Y., Pellicer, X. M., Pellitero, R., ... Woolridge, K. (2015). Manual mapping of drumlins in synthetic landscapes to assess operator effectiveness. *Journal of Maps*, 11(5), 719–729. <https://doi.org/10.1080/17445647.2014.957251>
- Howat, I. M., Porter, C., Smith, B. E., Noh, M.-J., & Morin, P. (2019). The reference elevation model of Antarctica. *The Cryosphere*, 13(2), 665–674. <https://doi.org/10.5194/tc-13-665-2019>
- Jamieson, S. S. R., Sugden, D. E., & Hulton, N. R. J. (2010). The evolution of the subglacial landscape of Antarctica. *Earth and Planetary Science Letters*, 293(1), 1–27. <https://doi.org/10.1016/j.epsl.2010.02.012>
- Kanamaru, T., Sukanuma, Y., Oiwane, H., Miura, H., Miura, M., Okuno, J., & Hayakawa, H. (2018). The weathering of granitic rocks in a hyper-arid and hypothermal environment: A case study from the Sør-Rondane Mountains, East Antarctica. *Geomorphology*, 317, 62–74. <https://doi.org/10.1016/j.geomorph.2018.05.015>
- Kehrl, L., Conway, H., Holschuh, N., Campbell, S., Kurbatov, A. V., & Spaulding, N. E. (2018). Evaluating the duration and continuity of potential climate records from the Allan Hills Blue Ice Area, East Antarctica. *Geophysical Research Letters*, 45(9), 4096–4104. <https://doi.org/10.1029/2018GL077511>
- Kleman, J., & Stroeven, A. P. (1997). Preglacial surface remnants and Quaternary glacial regimes in northwestern Sweden. *Geomorphology*, 19(1–2), 35–54. [https://doi.org/10.1016/S0169-555X\(96\)00046-3](https://doi.org/10.1016/S0169-555X(96)00046-3)
- Lukas, S., Benn, D. I., Boston, C. M., Brook, M., Coray, S., Evans, D. J. A., Graf, A., Kellerer-Pirklbauer, A., Kirkbride, M. P., Krabbendam, M., Lovell, H., Machiedo, M., Mills, S. C., Nye, K., Reinardy, B. T. I., Ross, F. H., & Signer, M. (2013). Clast shape analysis and clast transport paths in glacial environments: A critical review of methods and the role of lithology. *Earth-Science Reviews*, 121, 96–116. <https://doi.org/10.1016/j.earscirev.2013.02.005>
- Mackintosh, A. N., Verleyen, E., O’Brien, P. E., White, D. A., Jones, R. S., McKay, R., Dunbar, R., Gore, D. B., Fink, D., Post, A. L., Miura, H., Leventer, A., Goodwin, I., Hodgson, D. A., Lilly, K., Crosta, X., Golledge, N. R., Wagner, B., Berg, S., ... Massé, G. (2014). Retreat history of the East Antarctic Ice Sheet since the Last Glacial Maximum. *Quaternary Science Reviews*, 100, 10–30. <https://doi.org/10.1016/j.quascirev.2013.07.024>
- Näslund, J.-O. (2001). Landscape development in western and central Dronning Maud Land, East Antarctica. *Antarctic Science*, 13(3), 302–311. <https://doi.org/10.1017/S0954102001000438>
- Näslund, J. O., Fastook, J. L., & Holmlund, P. (2000). Numerical modelling of the ice sheet in western Dronning Maud Land, East Antarctica: Impacts of present, past and future climates. *Journal of Glaciology*, 46(152), 54–66. <https://doi.org/10.3189/172756500781833331>
- Newall, J. C. H., Dymova, T., Serra, E., Blomdin, R., Fredin, O., Glasser, N. F., ... Stroeven, A. P. (in submission). Mapping Antarctic glacial geomorphology from very high-resolution WorldView-2 and -3 satellite data. *Geomorphology*.
- Pour, A. B., Hashim, M., Hong, J. K., & Park, Y. (2019). Lithological and alteration mineral mapping in poorly exposed lithologies using Landsat-8 and ASTER satellite data: North-eastern Graham Land, Antarctic Peninsula. *Ore Geology Reviews*, 108, 112–133. <https://doi.org/10.1016/j.oregeorev.2017.07.018>

- Serra, E. (2017). Paleoglaciological study of the Ahlmannryggen, Borgmassivet and Kirwanveggen nunatak ranges, Dronning Maud Land, East Antarctica, using WorldView imagery. Master Thesis in Physical Geography and Quaternary Geology NKA190, Department of Physical Geography, Stockholm University, 66 p.
- Smith, M. J., & Wise, S. M. (2007). Problems of bias in mapping linear landforms from satellite imagery. *International Journal of Applied Earth Observation and Geoinformation*, 9(1), 65–78. <https://doi.org/10.1016/j.jag.2006.07.002>
- Spaulding, N. E., Spikes, V. B., Hamilton, G. S., Mayewski, P. A., Dunbar, N. W., Harvey, R. P., Schutt, J., & Kurbatov, A. V. (2012). Ice motion and mass balance at the Allan Hills blue-ice area, Antarctica, with implications for paleoclimate reconstructions. *Journal of Glaciology*, 58(208), 399–406. <https://doi.org/10.3189/2012JoG11J176>
- Stokes, C. R., Tarasov, L., Blomdin, R., Cronin, T. M., Fisher, T. G., Gyllencreutz, R., Hättestrand, C., Heyman, J., Hindmarsh, R. C. A., Hughes, A. L. C., Jakobsson, M., Kirchner, N., Livingstone, S. J., Margold, M., Murton, J. B., Noormets, R., Peltier, W. R., Peteet, D. M., Piper, D. J. W., ... Teller, J. T. (2015). On the reconstruction of palaeo-ice sheets: Recent advances and future challenges. *Quaternary Science Reviews*, 125, 15–49. <https://doi.org/10.1016/j.quascirev.2015.07.016>
- Stroeven, A. P., Hättestrand, C., Kleman, J., Heyman, J., Fabel, D., Fredin, O., Goodfellow, B. W., Harbor, J. M., Jansen, J. D., Olsen, L., Caffee, M. W., Fink, D., Lundqvist, J., Rosqvist, G. C., Strömberg, B., & Jansson, K. N. (2016). Deglaciation of Fennoscandia. *Quaternary Science Reviews*, 147, 91–121. <https://doi.org/10.1016/j.quascirev.2015.09.016>
- Sugden, D. E., Balco, G., Cowdery, S. G., Stone, J. O., & Sass III, L. C. (2005). Selective glacial erosion and weathering zones in the coastal mountains of Marie Byrd Land, Antarctica. *Geomorphology*, 67(3-4), 317–334. <https://doi.org/10.1016/j.geomorph.2004.10.007>
- Wentworth, C. K. (1922). A scale of grade and class terms for clastic sediments. *The Journal of Geology*, 30(5), 377–392. <https://doi.org/10.1086/622910>
- Zwinger, T., Schäfer, M., Martín, C., & Moore, J. C. (2014). Influence of anisotropy on velocity and age distribution at Scharffenbergbotnen blue ice area. *The Cryosphere*, 8(2), 607–621. <https://doi.org/10.5194/tc-8-607-2014>